SI Appendix

Crystal structure of *S. aureus* transglycosylase in complex with a lipid II analog and elucidation of peptidoglycan synthesis mechanism

Chia-Ying Huang[a,b], Hao-Wei Shih[a,c], Li-Ying Lin[a], Yi-Wen Tien[a], Ting-Jen Rachel Cheng[a], Wei-Chieh Cheng[a], Chi-Huey Wong[a,b,1], and Che Ma[a,b,1]

[a]Genomics Research Center, Academia Sinica, 128 Academia Road, Section 2, Taipei 115, Taiwan; [b]Institutes of Microbiology and Immunology, National Yang-Ming University, 155 Linong Street, Section 2, Taipei 112, Taiwan; and [c]Department of Chemistry, National Taiwan University, 1 Roosevelt Road, Section 4, Taipei 106, Taiwan

[1]To whom correspondence should be addressed. E-mail:chwong@gate.sinica.edu.tw (C.-H. W.) or cma@gate.sinica.edu.tw (C. M.)

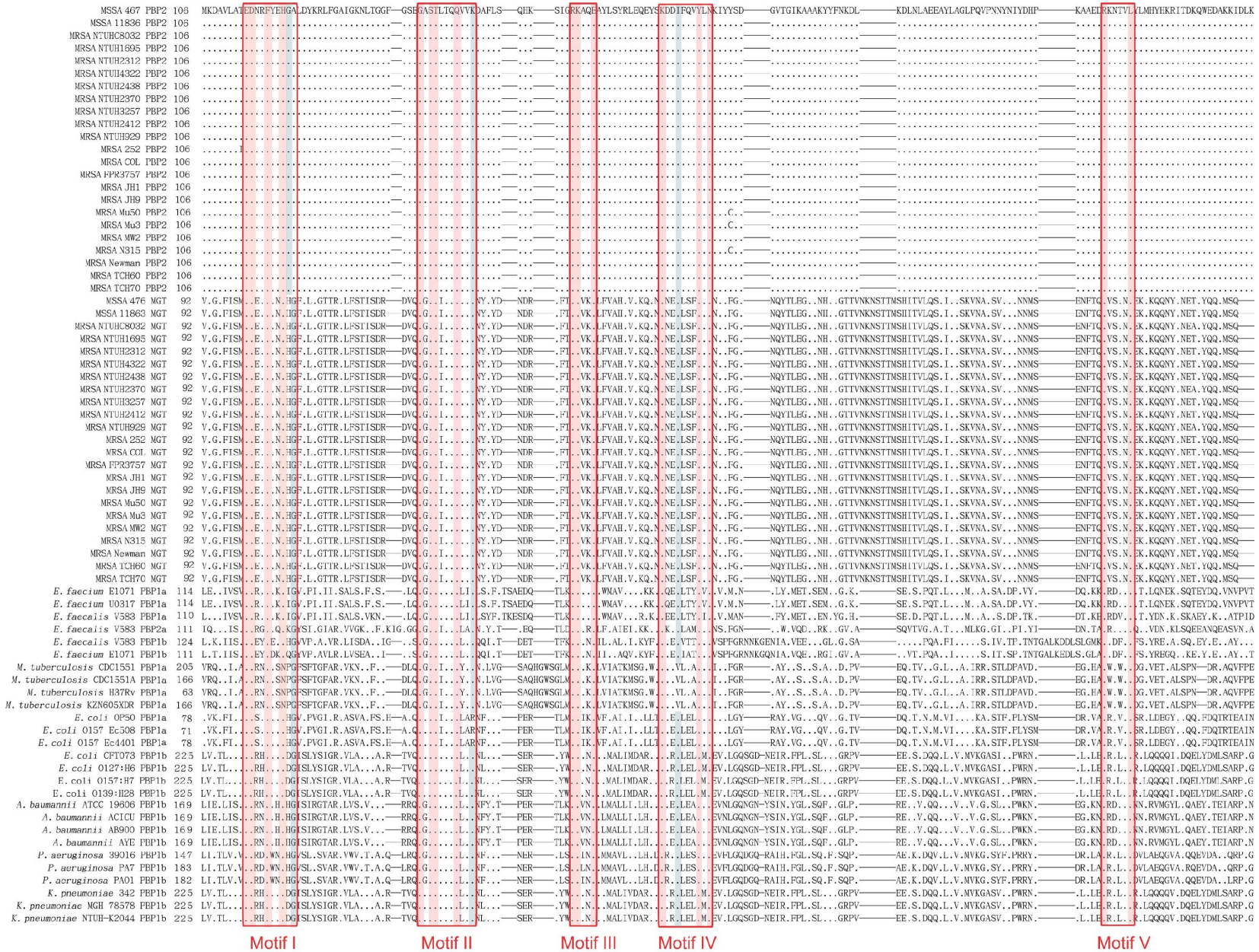
Motif I
Motif II
Motif III
Motif IV
Motif V

Fig. S1. TGs sequence alignments of different bacterial species. Residues are exactly identical in TG are shaded in red, and residues are highly conserved in TG are shaded in blue. The TG sequences were aligned using Jalview (1) software with the MAFFT multiple sequence alignment (2). PBP2 and MGT from MSSA 11836, MRSA NTUH1695, MRSA NTUH2312, MRSA NTUH4322, MRSA NTUH2438, MRSA NTUH2370, MRSA NTUH3257, MRSA NTUH2412 and MRSA NTUH929 are cloned and sequenced in this study.

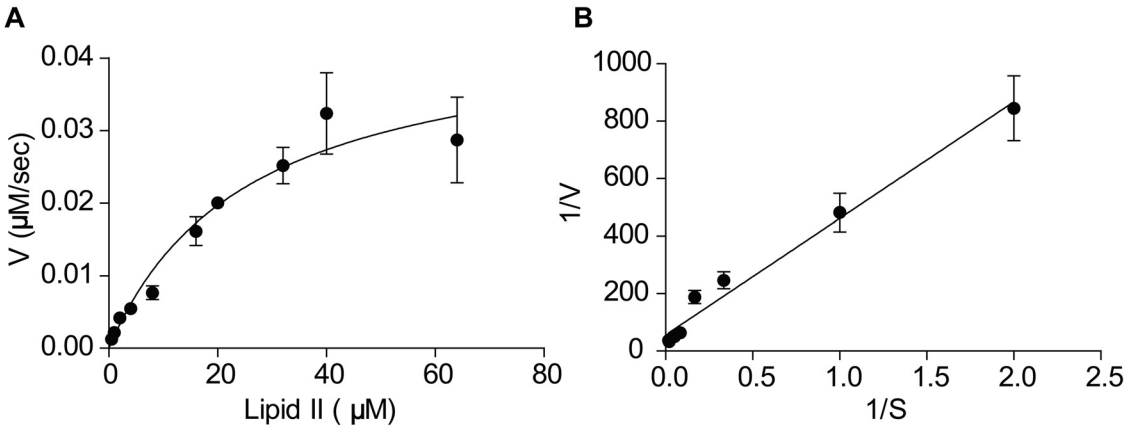

Fig. S2. SaMGT activity assay. (**A**) Saturation curve of SaMGT. The correlation between the concentration of substrate (NBD-Lipid II; *x* axis) and rate (V; *y* axis) is fitted into a curve. (**B**) Lineweaver–Burk plot with equation y = (405.6 ± 24.53) *x* + (56.1 ± 19.28). The activity of SaMGT is defined by measuring the consumption rate of NBD-lipid II. Following the Michaelis–Menten equation, $V_0 = V_{max}[S]/K_m + [S]$, the k_{cat} (s^{-1}) = 0.40 ± 0.063, K_m (μM) = 9.6 ± 0.76, and k_{cat} / K_m ($M^{-1}s^{-1}$) = (4.15 ± 0.46)*10^4. The figures are plotted by Prism 5.0. All experiments are performed at least three times, and standard deviations are shown.

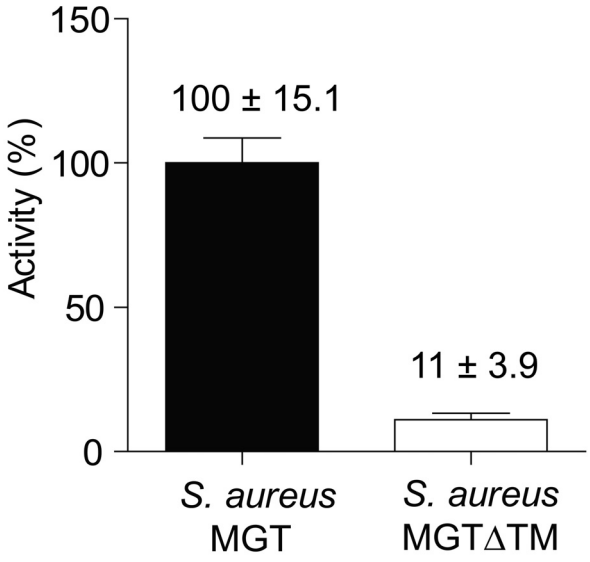

Fig. S3. Activity comparison of SaMGT and SaMGTΔTM. The activity of SaMGT is normalized to 100%. The figures are plotted by Prism 5.0. All experiments are performed at least three times, and standard deviations are shown.

A

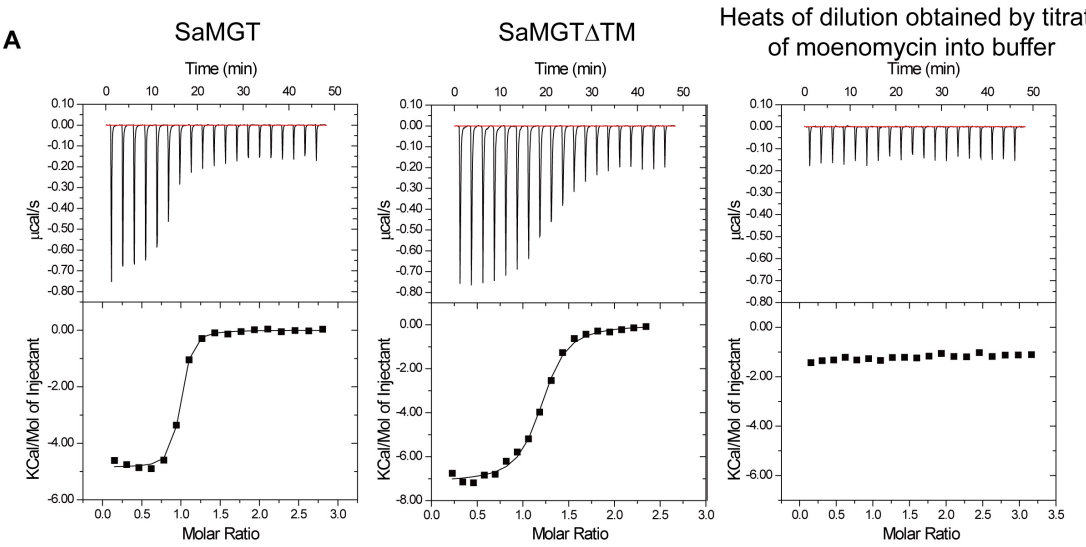

	SaMGT	SaMGTΔTM
Kd (μM)	0.19 ± 0.003	1.01 ± 0.01
ΔH (cal/mol)	-5009 ± 128	-6950 ± 30
-TΔS (cal/mol)	-4142 ± 129	-1224 ± 31
ΔG (cal/mol)	-9151 ± 257	-8174 ± 61

B

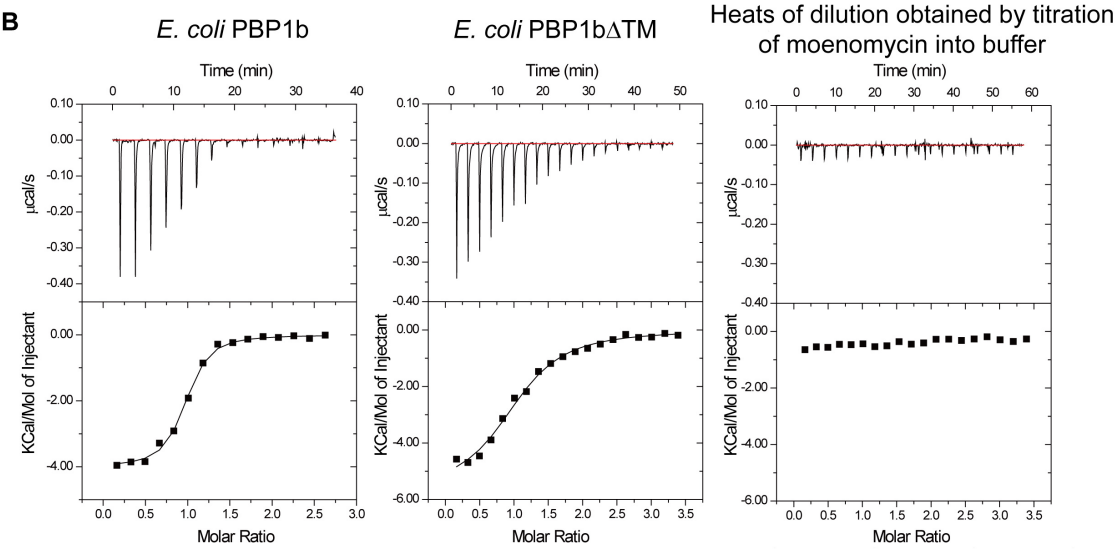

	E. coli PBP1b	*E. coli* PBP1bΔTM
Kd (μM)	0.71 ± 0.09	3.95 ± 0.24
ΔH (cal/mol)	-4396 ± 397	-5190 ± 51
-TΔS (cal/mol)	-3903 ± 457	-1873 ± 305
ΔG (cal/mol)	-8300 ± 70	-7198 ± 202

Fig. S4. Effect of TM helix of TG on moneomycin binding ability by using ITC. (**A**) Moenomycin is titrated in SaMGT (left panel), SaMGTΔTM (middle panel) or buffer (right panel). (**B**) Moenomycin is titrated in *E. coli* PBP1b (left panel), *E. coli* PBP1bΔTM (middle panel) or buffer (right panel). Following the Gibbs free energy $\Delta G = -RT \ln K = \Delta H - T\Delta S$ (where R is the gas constant and T is the absolute temperature), the standard free energy change (ΔG) and standard entropy change (ΔS) are calculated. The figures of ITC are plotted by MicroCal Origin version 5.0. All experiments are performed at least three times, and standard deviations are shown.

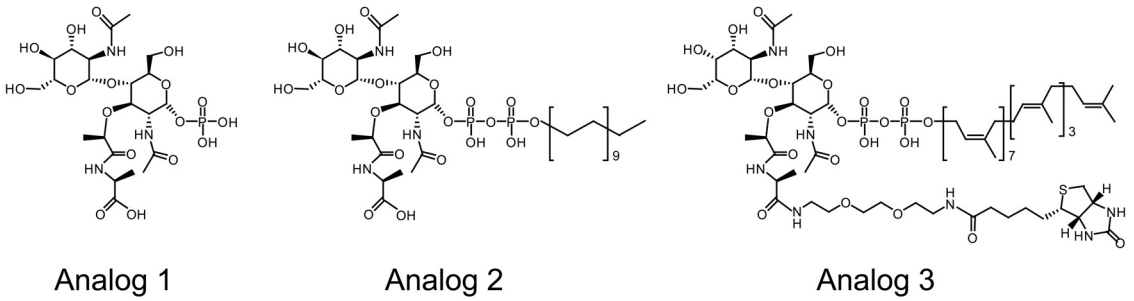

Fig. S5. Chemical structures of lipid II analogs. Three lipid II analogs with variant sugars, modified pentapeptide, and undecaprenyl moeity are made with ChemDraw (www.cambridgesoft.com).

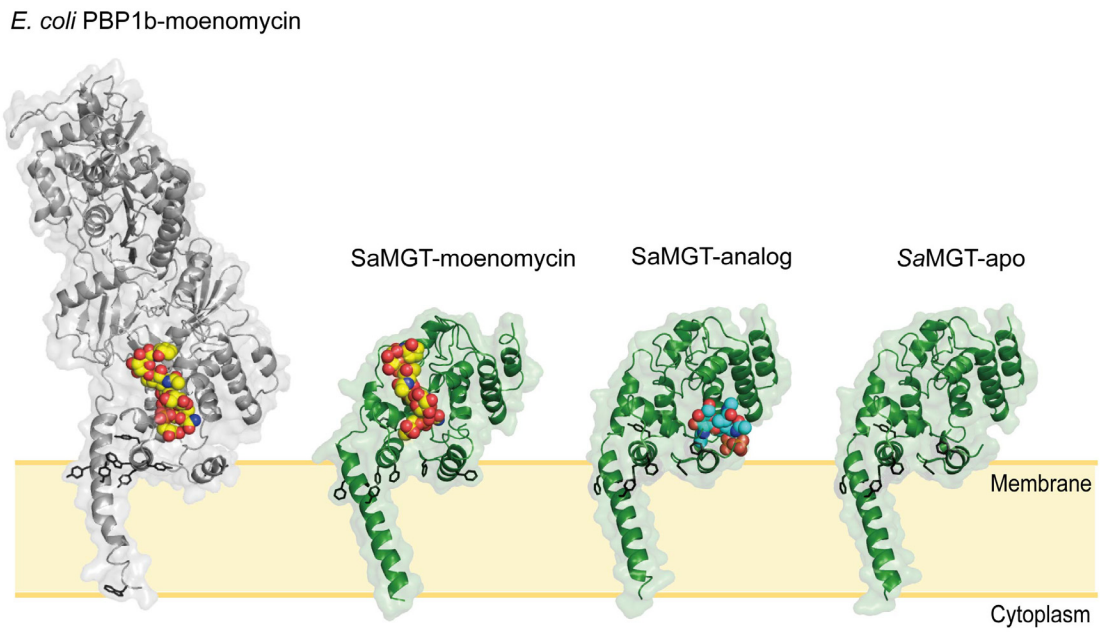

Fig. S6. The membrane-bound TGs reveal the similar orientation in the lipid bilayer. The structures of *E. coli* PBP1b and SaMGT are shown as ribbon in gray and green, respectively. Moenomycin and analog 3 are shown as van der Waals spheres in yellow and blue, respectively. Membrane interface is indicated by black stick of aromatic amino acid residues. Membrane and cytoplasm are indicated by orange lines.

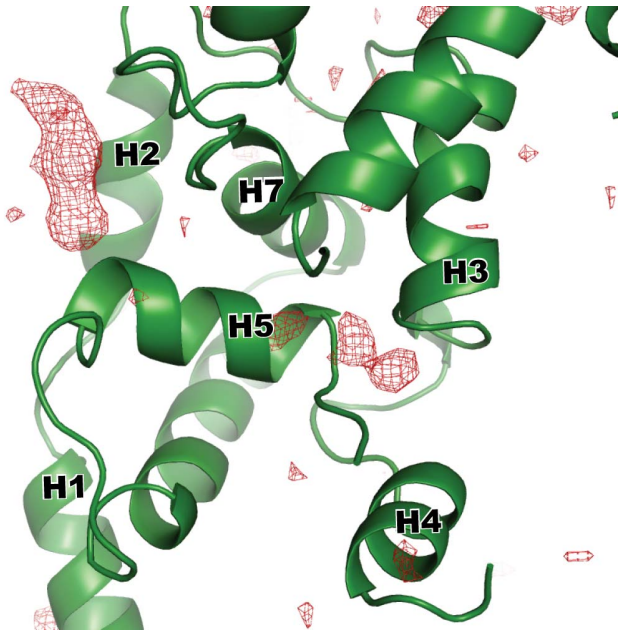

Fig. S7. An omit map of NBD-lipid II-deleted SaMGT-substrate. The omit map was generated from NBD-lipid II-deleted SaMGT model. The structure of SaMGT-substrate is shown as ribbon in green. The omit map for NBD-lipid II (σ–cutoff = 3 σ) is represented in red mesh. The helices of SaMGT-analog are indicated. We found two additional electron density patches. One overlaps with the analog 3 of the SaMGT-analog, which indicated that the analog 3 is located at the substrate binding site, and the other locates between H1, H5, and H7, which agreed with what we had proposed previously on the location of the polymerized glycan chain (3).

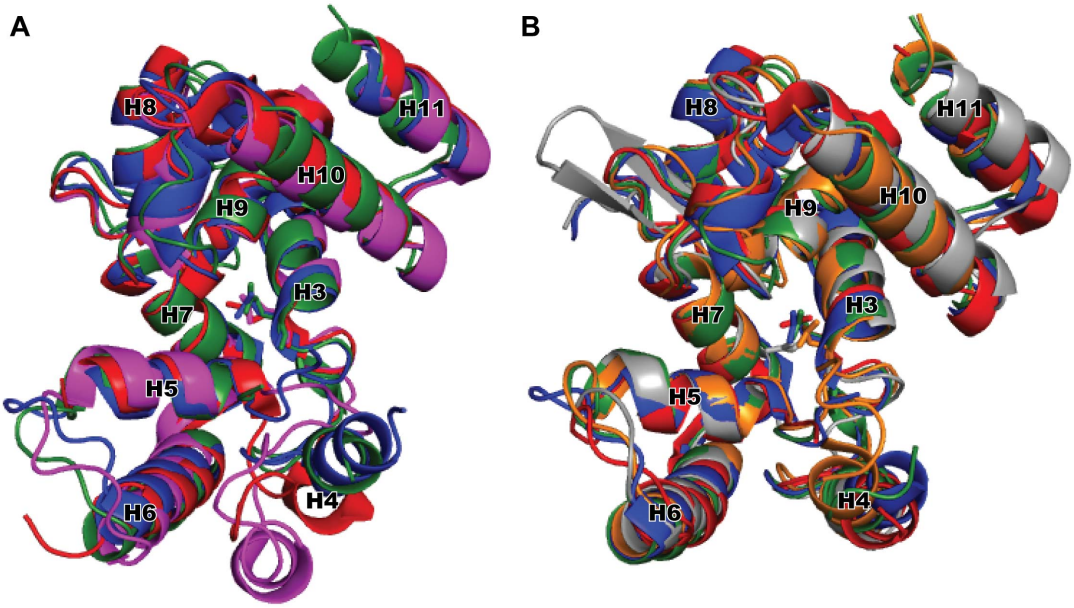

Fig. S8. Structural comparison of apo or ligand-bound TG. (**A**) Structural alignment of apo form TGs. Different TGs are represented in ribbon diagram. *A. aeolicus* PGT-apo (PDB ID code 2OQO), *S. aureus* PBP2-apo (PDB ID code 3DWK), *S. aureus* PBP2-apo (PDB ID code 2OLU), and SaMGT-apo are color-coded as blue, magenta, red, and green. (**B**) Structural alignment of ligand-bound TGs. *A. aeolicus* PGT-moenomycin (PDB ID code 3D3H), *S. aureus* PBP2-moenomycin (PDB ID code 2OLV), *E. coli* PBP1b-moenomycin (PDB ID code 3FWM), SaMGT-moenomycin, and SaMGT-analog are color-coded as blue, red, gray, orange, and green. Stick forms represent the conserved active sites of TGs. The numbers of helices on SaMGT are indicated.

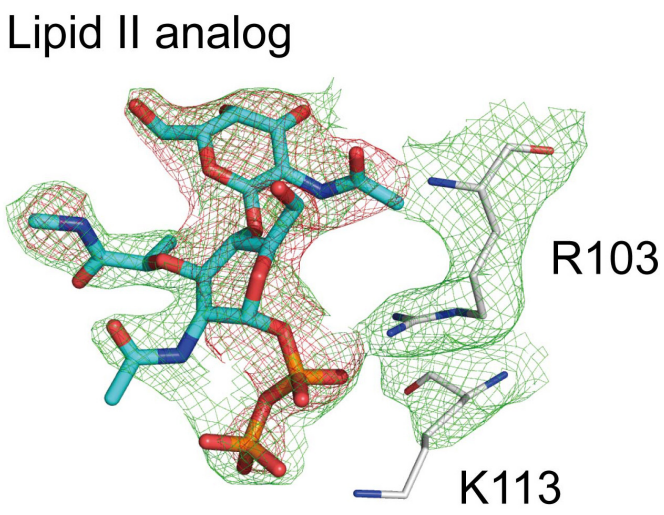

Fig. S9. Electron density map of the residues of SaMGT interact with pyrophosphate group of analog 3. The residues of SaMGT and analog 3 are shown as sticks in gray and blue, respectively. The 2Fo-Fc map for analog 3 and lipid II analog-contacting residues (σ–cutoff = 1 σ) are represented in green mesh. The omit map for analog 3 (σ–cutoff = 3 σ) is represented in red mesh.

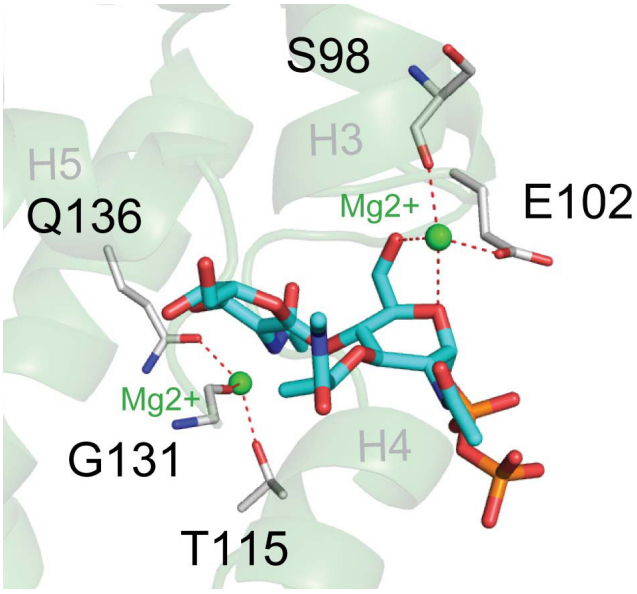

Fig. S10. Binding interaction between Mg^{2+}, analog 3, and SaMGT. The residues of SaMGT and analog 3 are shown as sticks in gray and blue, respectively. The Mg^{2+} cations are shown as balls in green. The Mg^{2+} cations can be identified in the electron density Fo-Fc map (σ–cutoff ~ 4.8σ), O···Mg···O angles (~ 90°), and Mg···O distances (~ 2.4 Å) in SaMGT-analog.

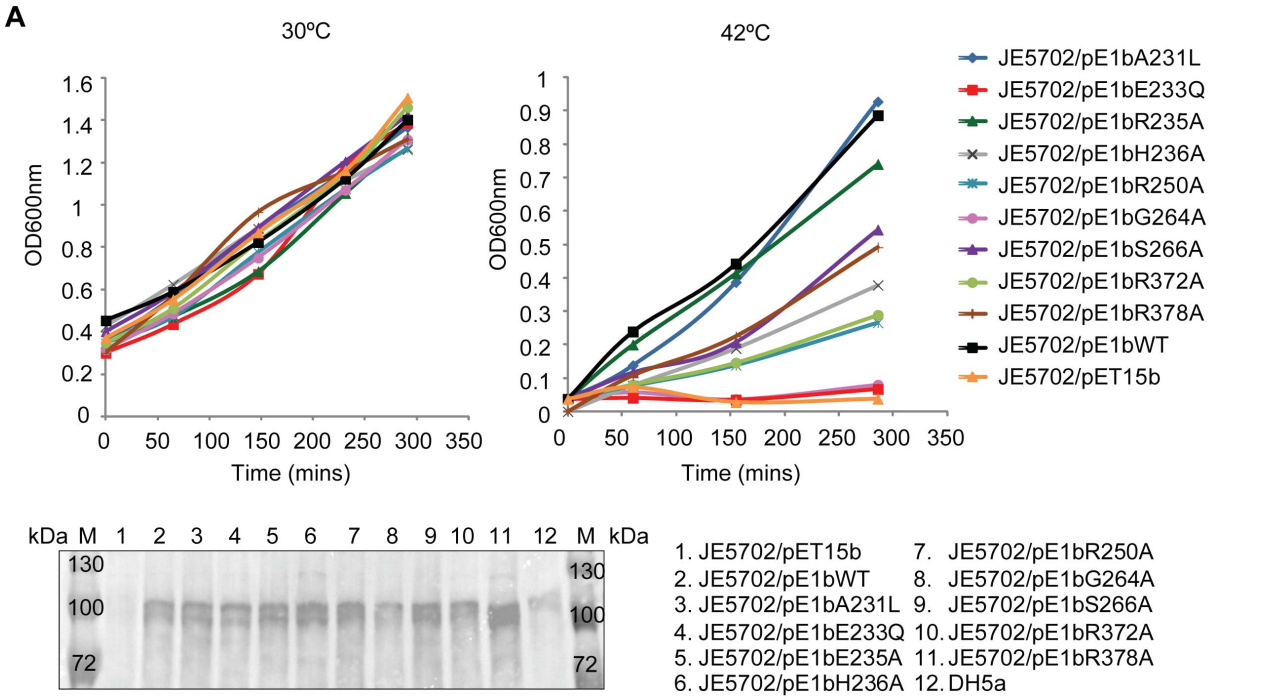
A
30ºC
42ºC
OD600nm
Time (mins)
JE5702/pE1bA231L
JE5702/pE1bE233Q
JE5702/pE1bR235A
JE5702/pE1bH236A
JE5702/pE1bR250A
JE5702/pE1bG264A
JE5702/pE1bS266A
JE5702/pE1bR372A
JE5702/pE1bR378A
JE5702/pE1bWT
JE5702/pET15b
kDa M 1 2 3 4 5 6 7 8 9 10 11 12 M kDa
130
100
72
1. JE5702/pET15b
2. JE5702/pE1bWT
3. JE5702/pE1bA231L
4. JE5702/pE1bE233Q
5. JE5702/pE1bE235A
6. JE5702/pE1bH236A
7. JE5702/pE1bR250A
8. JE5702/pE1bG264A
9. JE5702/pE1bS266A
10. JE5702/pE1bR372A
11. JE5702/pE1bR378A
12. DH5a

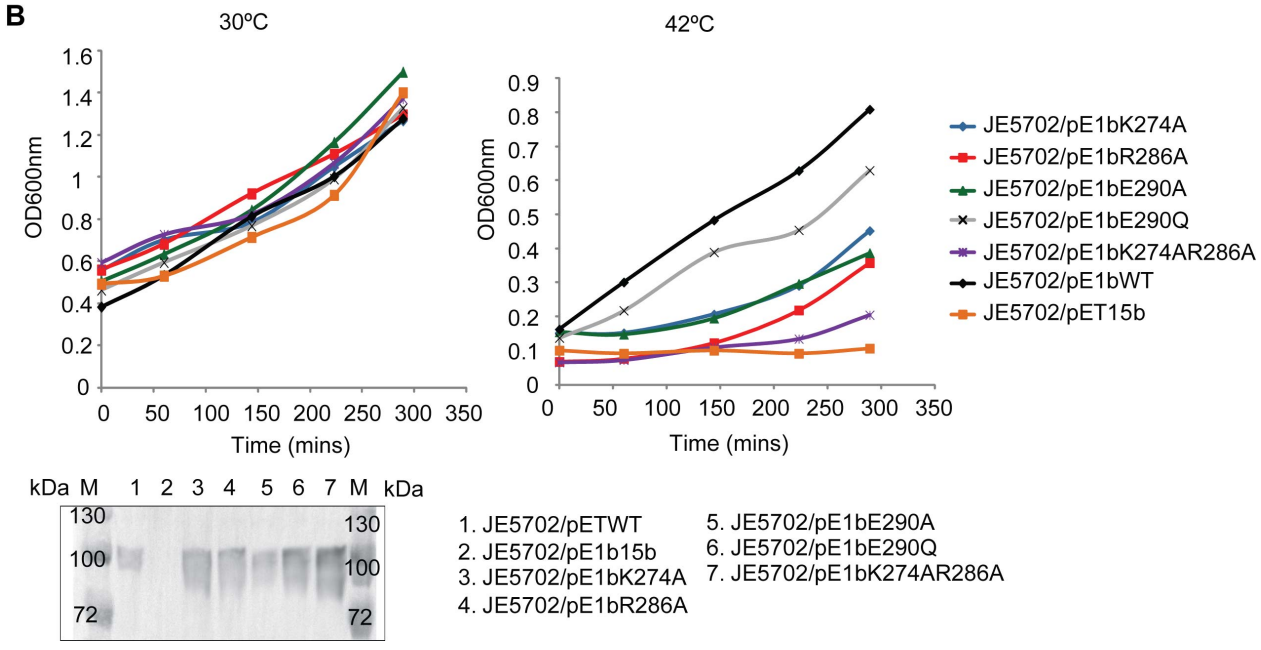
B
30ºC
42ºC
OD600nm
Time (mins)
JE5702/pE1bK274A
JE5702/pE1bR286A
JE5702/pE1bE290A
JE5702/pE1bE290Q
JE5702/pE1bK274AR286A
JE5702/pE1bWT
JE5702/pET15b
kDa M 1 2 3 4 5 6 7 M kDa
130
100
72
1. JE5702/pETWT
2. JE5702/pE1b15b
3. JE5702/pE1bK274A
4. JE5702/pE1bR286A
5. JE5702/pE1bE290A
6. JE5702/pE1bE290Q
7. JE5702/pE1bK274AR286A

Fig. S11. Complementary activity assay. Complementary activity of plasmids encoded non-mutated *E. coli* PBP1b (pE1bWT), lipid II analog-contacting residues mutated *E. coli* PBP1b (pE1bA231L, pE1bE233Q, pE1bR235A, pE1bH236A, pE1bR250A, pE1bG264A, pE1bS266A, pE1bR372A, and pE1bR378A), and residues of glyosyl donor site mutated *E. coli* PBP1b (pE1bK274A, pE1bR286A, pE1bE290A, pE1bE290Q, and pE1bK274AR286A) in *E. coli* JE5702 (PBP1b-defected/PBP1a-temperature-sensitive strain) at 30℃ and 42℃. Expression level of each mutant protein was shown below the complementary activity assay. The pE1bWT encodes the wild type *E. coli* PBP1b, which is positive control, and the pET15b is an empty vector, which is negative control, for the complementary activity assay. (**A**) Complementary activity of lipid II analog-contacting residues mutated *E. coli* PBP1b. (**B**) Complementary activity of residues of glyosyl donor site mutated *E. coli* PBP1b.

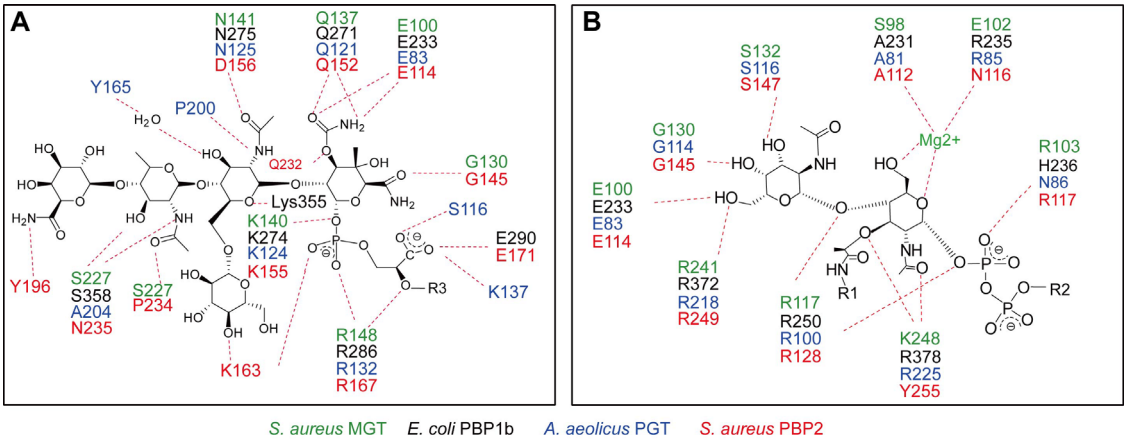

Fig. S12. Schematic view of interaction between TGs and moenomycin or lipid II analog 3. (**A**) Interaction between TGs and moenomycin. R1, R2 and R3 indicate the ala-diethylene glycol amine-biotin, undecaprenyl moiety and moenocinol moiety, respectively. (**B**) Interaction between TGs and lipid II analog 3. Hydrogen bonds (Distance $\leqq$ 3.5 Å) and interactions around Mg^{2+} are shown as dashed lines in red. Residues from SaMGT, *E. coli* PBP1b, *A. aeilocus* PGT, and *S. aureus* PBP2 are color-coded in green, black, blue and red, respectively. The residues aligned in the TG structures are indicated.

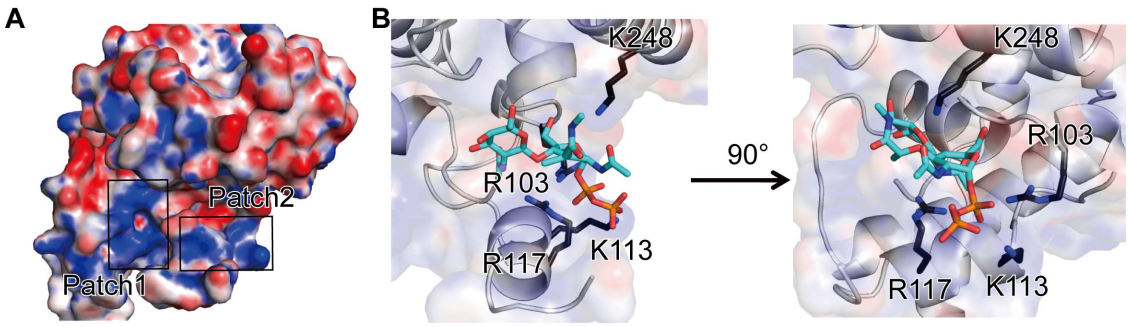

Fig. S13. Electrostatic surface representation of SaMGT. (**A**) Electrostatic surface of SaMGT binding pocket. The colors are coded by electrostatic potential from -18 kT/e (negative charge, red) to 18 kT/e (positive charge, blue), where k is the Boltzmann constant and T is absolute temperature. There are two positive charge patches; patch1 binds the phosphoric acid diester group of moenomycin, and patch2 binds the pyrophosphate group of analog 3. (**B**) Enlargement of patch2. The 80% surface transparency of (**A**). Two structures are shown in the same orientation, whereas the right panel is rotated 90°. The structure of SaMGT-analog is shown as ribbon in gray. The residues of positive charge around pyrophosphate are shown as sticks in black and residues numbers are indicated.

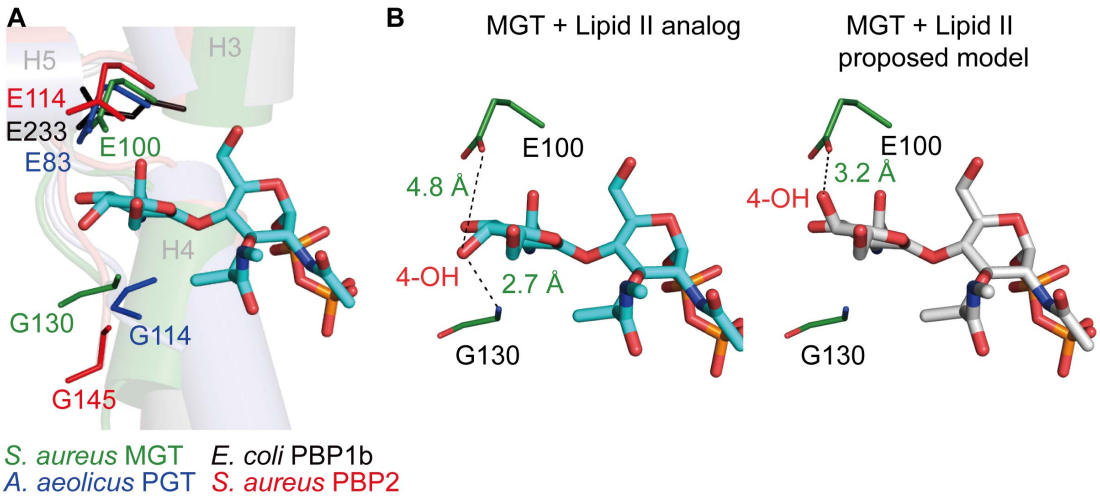

Fig. S14. Binding interaction between analog 3 and SaMGT and proposed mechanism for TG inhibition by analog 3. (**A**) Structural aligment of E100 and G130 in *Sa*MGT-analog with corresponding resdiues from *E. coli* PBP1b (PDB ID code 3FWM), *A. aeilocus* PGT (PDB ID code 3D3H), and *S. aureus* PBP2 (PDB ID code 2OLV). The colored code is the same as in **Fig. 3**. (**B**) Proposed mechanism for TG inhibition by analog 3. Analog 3 and lipid II are shown as sticks in blue and gray, respectively. Hydrogen bonds are shown as dashed lines in black.

Table S1 Data collection and refinement statistics

	SaMGT-apo	SaMGT-analog	SaMGT-substrate	SaMGT-moenomycin
Data collection				
Space group	$P2_12_12_1$	$P2_12_12_1$	$P2_12_12_1$	$P2_12_12$
Cell dimensions				
a, *b*, *c* (Å)	66.68, 67.41, 152.81	66.50, 67.43, 152.19	66.88, 67.16, 140.94	130.42, 52.85, 54.59
Resolution (Å)	30.00-2.5(2.59-2.50)[a]	30.00-2.3 (2.38-2.30)	30.00-3.2 (3.31-3.20)	30.00-3.66 (3.79-3.66)
No. of observations	159111	148910	76658	25587
No. of unique reflections	23658	30750	10888	4460
R_{sym}	10.2 (49.0)	5.7 (49.8)	8.8 (47.1)	4.2 (48.4)
$I / \sigma I$	19.1 (3.3)	4.9 (4.1)	20.4 (4.2)	15.3 (4.2)
Completeness (%)	99.4 (98.9)	98.5 (96.8)	99.6 (99.4)	99.0 (98.9)
Redundancy	6.7 (6.3)	4.9 (4.1)	7.0 (6.7)	7.7 (8.0)
Refinement statistics				
Resolution (Å)	2.5	2.3	3.2	3.6
No.of reflections	23609	30698	10845	4344
R_{work} / R_{free} (%)	20.3/25.7	19.9/24.2	26.5/33.0	30.4/30.9
No. atoms				
Protein	3661	3598	3565	1854
Ligand/ion	–/1	43/2	–/–	84/–
Water	46	52	–	–
B-factors				
Protein	85.8	87.5	132.2	176.1
Ligand/ion	–/91.8	103.9/89.7	–/–	193.7/–
Water	56.9	60.3	–	–
R.m.s. deviations				
Bond lengths (Å)	0.013	0.019	0.006	0.005
Bond angles (°)	0.84	0.93	1.02	1.13
Ramachandran plot				
Favored/allowed/disallowed (%)	91.3/8.7/0	89.8/10.2/0	84.1/15.9/0	82.6/16.9/0.5

[a]Values in parentheses are for the highest-resolution shell. Each dataset was collected from a single crystal.

SUPPLEMENTARY REFERENCES

1. Clamp M, Cuff J, Searle SM, & Barton GJ (2004) The Jalview Java alignment editor. *Bioinformatics* 20:426-427.
2. Katoh K, Kuma K, Toh H, & Miyata T (2005) MAFFT version 5: improvement in accuracy of multiple sequence alignment. *Nucleic Acids Res* 33:511-518.
3. Sung MT*, et al.* (2009) Crystal structure of the membrane-bound bifunctional transglycosylase PBP1b from Escherichia coli. *Proc Natl Acad Sci USA* 106:8824-8829.